J|A|C|S
ARTICLES
Published on Web 09/10/2004

Analysis of the Conserved P9-G10.1 Metal-Binding Motif in Hammerhead Ribozymes with an Extra Nucleotide Inserted between A9 and G10.1 Residues

Masaki Warashina,[†] Tomoko Kuwabara,[†,‡] Yuka Nakamatsu,[†] Yasuomi Takagi,[†,#] Yoshio Kato,[†,‡] and Kazunari Taira*[,†,‡]

Contribution from the Gene Function Research Center, National Institute of Advanced Industrial Science and Technology (AIST), Central 4, 1-1-1 Higashi, Tsukuba Science City 305-8562, Japan, Department of Chemistry and Biotechnology, School of Engineering, The University of Tokyo, Hongo, Tokyo 113-8656, Japan, and iGENE Therapeutics, Inc., c/o AIST, Central 4, 1-1-1 Higashi, Tsukuba Science City 305-8562, Japan

Received January 21, 2004; E-mail: taira@chembio.t.u-tokyo.ac.jp

Abstract: Hammerhead ribozymes (Rz) have catalytically important tandem G:A pairs in the core region, and we recently demonstrated that the P9-G10.1 motif (a sheared-type G:A pair with a guanine residue on the 3′ side of the adenine residue) with several flanking base pairs is sufficient for capture of divalent cations, such as Mg^{2+} and Cd^{2+} ions that are important to maintain full activities (Tanaka et al. *J. Am. Chem. Soc.* **2002**, *124*, 4595−4601; Tanaka et al. *J. Am. Chem. Soc.* **2004**, *126*, 744−752). We also found that mutant hammerhead ribozymes that have an additional G residue inserted between A9 and G10.1 residues (the metal-binding P9-G10.1 motif) have significant catalytic activities. In this study, we demonstrate that the hammerhead ribozymes are capable of maintaining the catalytically competent structure even when the tandem, sheared-type G:A pairs were perturbed by an insertion of an additional nucleotide, whereas the chirality of the phosphorothioate at the P9 position significantly influenced the enzymatic activity for both the natural and G-inserted ribozymes.

Introduction

The hammerhead ribozyme is one of the smallest RNA enzymes. Because of its small size and potential utility as an antiviral agent, it has been extensively investigated in terms of the mechanism of its action[1−4] and possible applications in vivo.[5] It was first recognized as the sequence motif responsible for self-cleavage (cis action) in the satellite RNAs of certain viruses.[6] The putative consensus sequence required for activity has three duplex stems and a conserved "core" of two nonhelical segments, plus an unpaired nucleotide at the cleavage site (Figure 1). The trans-acting ribozyme consists of an antisense section (stems I and III) and a catalytic domain with a flanking stem/loop II section (hereafter, the term ribozymes, Rz, refers exclusively to hammerhead ribozymes unless otherwise noted).[7] Stem II can be a common stem in the case of dimeric maxizymes.[8] Such RNA motifs can cleave oligoribonucleotides at specific sites.[9] In nature, the most commonly found cleavage

[†] National Institute of Advanced Industrial Science and Technology (AIST).
[‡] The University of Tokyo.
[#] iGENE Therapeutics, Inc.

(1) (a) Dahm, S. C.; Uhlenbeck, O. C. *Biochemistry* **1991**, *30*, 9464−9469. (b) Dahm, S. C.; Derrick, W. B.; Uhlenbeck, O. C. *Biochemistry* **1993**, *32*, 13040−13045. (c) Pyle, A. M. *Science* **1993**, *261*, 709−714. (d) Hertel, K. J.; Herschlag, D.; Uhlenbeck, O. C. *Biochemistry* **1994**, *33*, 3374−3385. (e) Sawata, S.; Komiyama, M.; Taira, K. *J. Am. Chem. Soc.* **1995**, *117*, 2357−2358. (f) Baidya, N.; Uhlenbeck, O. C. *Biochemistry* **1997**, *36*, 1108−1114. (g) Birikh, K. R.; Heaton, P. A.; Eckstein, F. *Eur. J. Biochem.* **1997**, *245*, 1−16. (h) Hertel, K. J.; Peracchi, A.; Uhlenbeck, O. C.; Herschlag, D. *Proc. Natl. Acad. Sci. U.S.A.* **1997**, *94*, 8497−8502. (i) Pontius, B. W.; Lott, W. B.; von Hippel, P. H. *Proc. Natl. Acad. Sci. U.S.A.* **1997**, *94*, 2290−2294. (j) Lott, W. B.; Pontius, B. W.; von Hippel, P. H. *Proc. Natl. Acad. Sci. U.S.A.* **1998**, *95*, 542−547. (k) Stage-Zimmermann, T.; Uhlenbeck, O. C. *RNA* **1998**, *4*, 875−889. (l) Zhou, D.-M.; Taira, K. *Chem. Rev.* **1998**, *98*, 991−1026. (m) Warashina, M.; Takagi, Y.; Stec, W. J.; Taira, K. *Curr. Opin. Biotechnol.* **2000**, *11*, 354−362.
(2) Scott, E. C.; Uhlenbeck, O. C. *Nucleic Acids Res.* **1999**, *27*, 479−484.
(3) (a) Wang, S.; Karbstein, K.; Peracchi, A.; Beigelman, L.; Herschlag, D. *Biochemistry* **1999**, *38*, 14363−14378. (b) Murray, J. B.; Scott, W. G. *J. Mol. Biol.* **2000**, *296*, 33−41. (c) Murray, J. B.; Szoke, H.; Szoke, A.; Scott, W. G. *Mol. Cell* **2000**, *5*, 279−287. (d) O'Rear, J. L.; Wang, S.; Feig, A. L.; Beigelman, L.; Uhlenbeck, O. C.; Herschlag, D. *RNA* **2001**, *7*, 537−545.
(4) Yoshinari, K.; Taira, K. *Nucleic Acids Res.* **2000**, *28*, 1730−1742.
(5) (a) Sarver, N.; Cantin, E. M.; Chang, P. S.; Zaia, J. A.; Lande, P. A.; Stephens, D. A.; Rossi, J. J. *Science* **1990**, *247*, 1222−1225. (b) Thompson, J. D.; Macejak, D.; Couture, L.; Stinchcomb, D. T. *Nature Med.* **1995**, *1*, 277−278. (c) Tuschl, T.; Thomson, J. B.; Eckstein, F. *Curr. Opin. Struct. Biol.* **1995**, *5*, 296−302. (d) Kawasaki, H.; Ohkawa, J.; Tanishige, N.; Yoshinari, K.; Murata, T.; Yokoyama, K. K.; Taira, K. *Nucleic Acids Res.* **1996**, *24*, 3010−3016. (e) Kato, Y.; Kuwabara, T.; Warashina, M.; Toda, H.; Taira, K. *J. Biol. Chem.* **2001**, *276*, 15378−15385. (f) Kawasaki, H.; Onuki, R.; Suyama, E.; Taira, K. *Nat Biotechnol.* **2002**, *20*, 376−380. (g) Nelson, L.; Suyama, E.; Kawasaki, H.; Taira, K. *Targets* **2003**, *2*, 191−200.
(6) (a) Hutchins, C. J.; Rathjen, P. D.; Forster, A. C.; Symons, R. H. *Nucleic Acids Res.* **1986**, *14*, 3627−3640. (b) Symons, R. H. *Trends Biochem. Sci.* **1989**, *14*, 445−450.
(7) (a) Uhlenbeck, O. C. *Nature* **1987**, *328*, 596−600. (b) Haseloff, J.; Gerlach, W. L. *Nature* **1988**, *334*, 585−591.
(8) (a) Amontov, S.; Taira, K. *J. Am. Chem. Soc.* **1996**, *118*, 1624−1628. (b) Kuwabara, T.; Amontov, S.; Warashina, M.; Ohkawa, J.; Taira, K. *Nucleic Acids Res.* **1996**, *24*, 2302−2310. (c) Kuwabara, T.; Warashina, M.; Orita, M.; Koseki, S.; Ohkawa, J.; Taira, K. *Nature Biotechnol.*, **1998**, *16*, 961−965. (d) Kuwabara, T.; Warashina, M.; Tanabe, T.; Tani, K.; Asano, S.; Taira, K. *Mol. Cell*, **1998**, *2*, 617−627. (e) Tanabe, T.; Kuwabara, T.; Warashina, M.; Tani, K.; Taira, K.; Asano, S. *Nature* **2000**, *406*, 473−474.

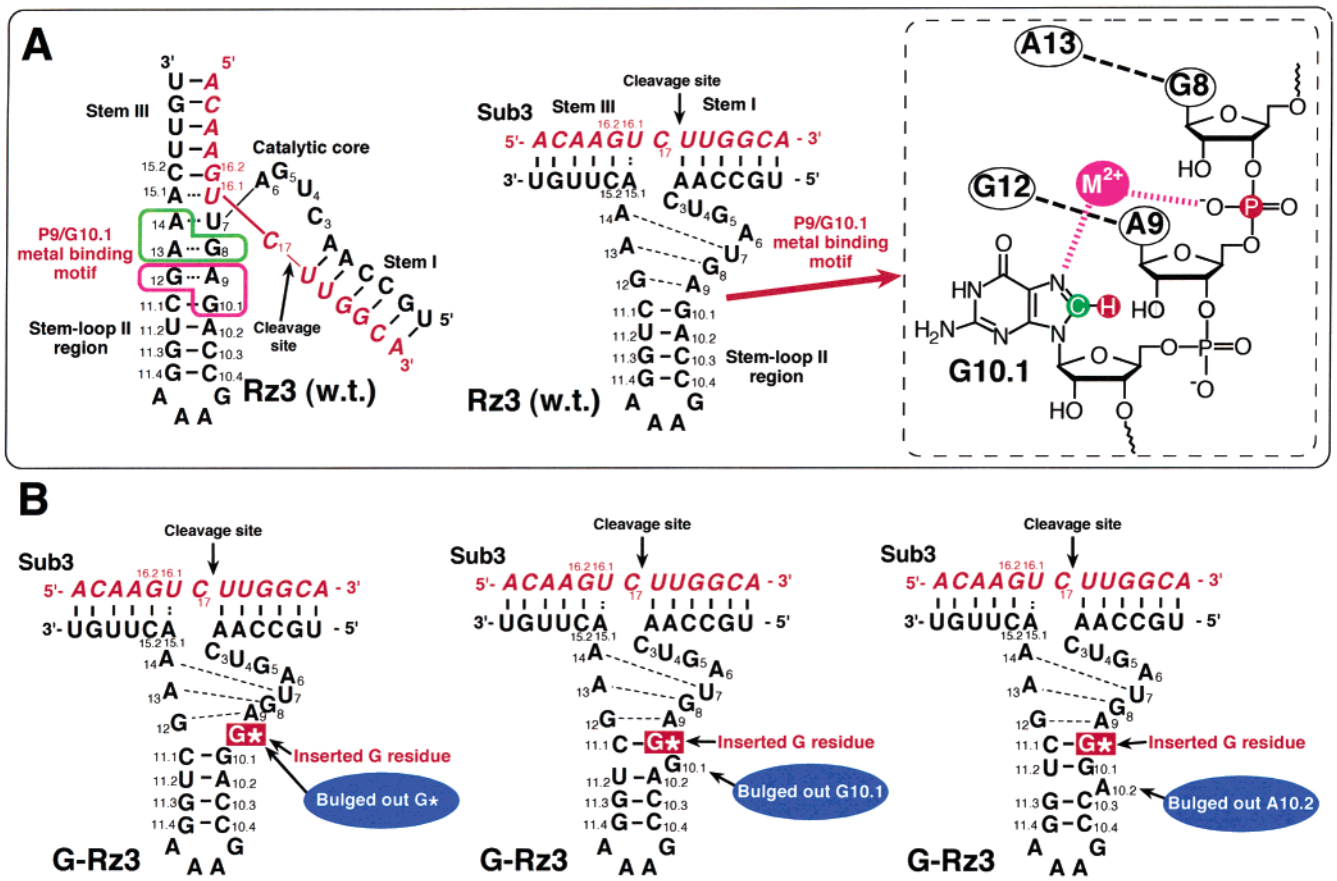

Figure 1. (A) Secondary structures of the hammerhead ribozyme. (Right) Schematic representation of the P9-G10.1 motif, as revealed by X-ray crystallography. A divalent ion is shown in magenta, and is linked to binding sites via magenta dashed lines. The tandem G:A pairs are indicated by black dashed lines with residue names. (B) Possible secondary structures of the G-inserted mutant hammerhead ribozymes. The bulged-out nucleobases are different, and the inserted G nucleotide is indicated with an asterisk. The substrate-recognition sequence is identical in both Rz3 and G-Rz3.

triplet is GUC, though GUA and AUA also have been observed. Mutagenesis studies have revealed that cleavage triplets of the NUX rule are tolerated (where N is any nucleotide and X is either A, U, or C).

Activities of hammerhead ribozymes (Rz) are heavily dependent on divalent metal ions, and these ribozymes use divalent ions as the catalytic cofactors, at least under physiological conditions.[3,10] X-ray crystallography has revealed that metal ions bind to core sequences that include tandem G:A pairs[11] (Figure 1A). In most crystal structures analyzed, metal ions bound at the tandem G−A pairs through the phosphate of A9 (P9) and N7 of G10.1 (P9-G10.1 motif, enclosed by the magenta line in Figure 1A), and more recent NMR analyses demonstrated that the nature of the interaction at the P9-G10.1 motif is an inner-sphere coordination, namely, the P9 metal ion binds directly to the N7 of G10.1.[11d] NMR spectroscopy of a Rz in solution also revealed another metal-binding site, namely, the phosphate of A13.[12] This site has structural features similar to those of the P9-G10.1 motif of Rz (enclosed by the green line in Figure 1A), and the sheared-type G−A pair with a purine residue on the 3′ side of the adenine appears to be a general metal-binding motif.[11c,d] Furthermore, it was once suggested that a metal ion bound to the P9-G10.1 motif might be a catalytic metal ion,[3] and it is obviously important to characterize this motif and its properties. On the basis of NMR analysis, we recently demonstrated that the P9-G10.1 motif can, by itself, support the binding of the structurally and catalytically important Cd^{2+} ion as well as other general divalent cations in solution.[11,12]

To determine whether other sequences might be possible in the hammerhead's catalytic core, attempts were made to select functional Rz sequences in vitro and in vivo from a population of random sequences.[13] However, such selection studies indi-

(9) (a) Ruffer, D. E.; Stormo, G. D.; Uhlenbeck, O. C. *Biochemistry* **1990**, *29*, 10695−10702. (b) Shimayama, T.; Nishikawa, S.; Taira, K. *Biochemistry* **1995**, *34*, 3649−3654.
(10) (a) Lilley, D. M. J. *Curr. Opin. Struct. Biol.* **1999**, *9*, 330−338. (b) Takagi, Y.; Warashina, M.; Stec, W. J.; Yoshinari, K.; Taira, K. *Nucleic Acids Res.* **2001**, *29*, 1815−1834. (c) Zhou, J. M.; Zhou, D. M.; Takagi, Y.; Kasai, Y.; Inoue, A.; Baba, T.; Taira, K. *Nucleic Acids Res.* **2002**, *30*, 2374−2382. (d) Inoue, A.; Takagi, Y.; Taira, K. *Nucleic Acids Res.* **2004**, *32*, 4217−4223. (e) Takagi, Y.; Inoue, A.; Taira, K. *J. Am. Chem. Soc.*, published online Sep 11, 2004 http://dx.doi.org/10.1021/ja031991u.
(11) (a) Pley, H. W.; Flaherty, K. M.; McKay, D. B. *Nature* **1994**, *372*, 68−74. (b) Scott, W. G.; Finch, J. T.; Klug, A. *Cell* **1995**, *81*, 991−1002. (c) Tanaka, Y.; Kojima, C.; Morita, E. H.; Kasai, Y.; Tanaka, T.; Taira, K. *J. Am. Chem. Soc.* **2002**, *124*, 4595−4601. (d) Tanaka, Y.; Kasai, Y.; Mochizuki, S.; Wakisaka, A.; Morita, E. H.; Kojima, C.; Toyozawa, A.; Kondo, Y.; Taki, M.; Takagi, Y.; Inoue, A.; Yamazaki, K.; Taira, K. *J. Am. Chem. Soc.* **2004**, *126*, 744−752.
(12) (a) Hansen, M. R.; Simorre J.-P.; Hanson, P.; Mokler, V.; Bellon, L.; Beigelman, L.; Pardi, A. *RNA* **1999**, *5*, 1099−1104. (b) Tanaka, Y.; Morita, E. H.; Hayashi, H.; Kasai, Y.; Tanaka, T.; Taira, K. *J. Am. Chem. Soc.* **2000**, *122*, 11303−11310. (c) Maderia, M., Hunsicker, L. M.; DeRose, V. J. *Biochemistry* **2000**, *39*, 12113−12120.
(13) (a) Long, D. M.; Uhlenbeck, O. C. Proc. *Natl. Acad. Sci. U.S.A.* **1994**, *91*, 6977−6981. (b) Ishizaka, M.; Ohshima, Y.; Tani, T. *Biochem. Biophys. Res. Commun.* **1995**, *214*, 403−409. (c) Thomson, J. B.; Sigurdsson S. T.; Zeuch, A.; Eckstein, F. *Nucleic Acids Res.* **1996**, *24*, 4401−4406. (d) Vaish, N. K.; Heaton, P. A.; Eckstein, F. *Biochemistry* **1997**, *36*, 6495−6501. (e) Fujita, S.; Koguma, T.; Ohkawa, J.; Mori, K.; Kohda, T.; Kise, H.; Nishikawa, S.; Iwakura, M.; Taira, K. *Proc. Natl. Sci. Acad. U.S.A.* **1997**, *94*, 391−396. (f) Kore, A. R.; Vaish, N. K.; Morris, J. A.; Eckstein, F. *J. Mol. Biol.* **2000**, *301*, 1113−1121.

cated that the consensus sequence, derived from viruses and virusoids, was the optimal sequence.[13c,d] However, other data suggested that mutant Rz, with one extra nucleotide insertion into the above-mentioned metal-binding P9-G10.1 motif, comprising A9 and G10.1 residues, supported the cleavage activity.[5d,14] This was a surprise to us because attempts in the past had failed to isolate any mutant ribozymes that had catalytic activities comparable to that of the wild-type ribozyme.[13]

Although there exist natural ribozymes that have an extra nucleotide inserted between the A9 and G10.1 residues,[14a−c,f] the nature of the important P9 metal coordination within the nucleotide-inserted P9-G10.1 motif remains unclear. In this report, we examined several types of extra nucleotide-inserted ribozymes. We found that one type of G-Rz (G-Rz3; G-inserted mutant ribozyme) had catalytic power with a k_{cat} value of 6.4 min^{-1} in 50 mM Tris-HCl (pH 8.0) and 10 mM $MgCl_2$. To the best of our knowledge, this and another U-inserted Rz have the highest k_{cat} values ever reported for a mutant ribozyme with natural components.[14e,f] More importantly, structural and kinetic analyses on these extra nucleotide-inserted mutant Rz revealed that the original stem II, which includes the G10.1:C11.1 pair, was maintained in the mutants and the original P9 phosphate (the phosphate between G8 and A9) still plays the pivotal role in the establishment of the active Rz core. These results suggest that the P9 metal ion is important in establishing the active Rz structure, but other alternative structures involving the sheared-type G:A pairs are also possible to support the catalysis in full.

Experimental Section

Synthesis of Ribozymes and Substrates. Ribozymes (Rz2 and Rz3; Figure 1A), extra nucleotide-inserted mutant ribozymes [G-Rz1−G-Rz4 (Figure 2A), C-, A-, U-, and $C_{10.1}$:$G_{11.1}$−Rz3 (Figure 4), and Rz3S (Figure 5A)], and their corresponding substrates (Sub1−Sub4; Figure 2A) were chemically synthesized on a DNA/RNA synthesizer (model 394; Perkin-Elmer, Applied Biosystems, Foster City, CA). Sub1 contained a GUU triplet located at nt 1168 of the p300 mRNA (Figure 2).[15] Sub2, Sub3, and Sub4 contained, respectively, GUA at nt 1181, GUC at 1401, and GUA at 1412 (Figure 2A). Reagents for RNA synthesis were purchased from Perkin-Elmer, Applied Biosystems. Oligonucleotides were purified as described in the user bulletin from ABI (no. 53; 1989) with minor modifications. Further purification was based on polyacrylamide gel electrophoresis as described previously.[16]

Kinetic Measurements. The kinetic parameters shown in Figure 2A were determined basically in 10 mM $MgCl_2$ and 50 mM Tris-HCl (pH 8.0; except for the pH−rate profile) under substrate-saturating (multiple-turnover) conditions at 37 °C. Reactions were initiated by the addition of $MgCl_2$ to a buffered solution that contained the ribozyme (20 nM) together with the substrate (from 100 nM to 10 μM), and each resultant mixture was then incubated at 37 °C. The 5′ terminus of each substrate was labeled with [γ-^{32}P]ATP using T4 polynucleotide kinase (Takara Shuzo, Tokyo).

Profiles of log(k_{obs}) vs pH were obtained under conditions similar to saturating conditions. The concentrations of ribozyme and substrate were 20 nM and 5 μM, respectively. The reactions were examined at pH 7.0, 7.5, and 8.0.

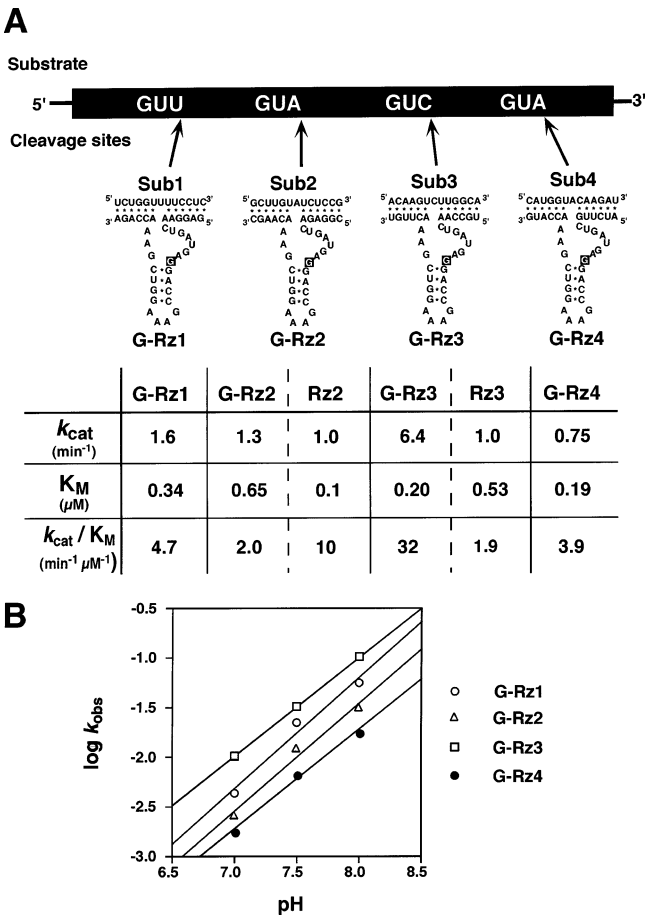

	G-Rz1	G-Rz2	Rz2	G-Rz3	Rz3	G-Rz4
k_{cat} (min^{-1})	1.6	1.3	1.0	6.4	1.0	0.75
K_M (μM)	0.34	0.65	0.1	0.20	0.53	0.19
k_{cat} / K_M (min^{-1} μM^{-1})	4.7	2.0	10	32	1.9	3.9

Figure 2. (A) Sequences of G-inserted mutant hammerhead ribozymes and their target sites within the gene for p300. Sequences of their substrates used in kinetic measurements are also shown. Kinetic parameters of cleavage of original Rz and G-Rz are summarized in the table. (B) pH−log k_{obs} of mutant G-Rz. The slope of this profiles are the same, about 1.0.

The rate constants shown in Figure 4B were measured in 50 mM Tris-HCl (pH 8.0) and 25 mM $MgCl_2$, under multiple-turnover conditions at 37 °C. The rate constant of $C_{10.1}$:$G_{11.1}$−Rz3 (Figure 4) was measured in 50 mM Tris-HCl (pH 8.0) and 25 mM $MgCl_2$, under a single-turnover condition because of the low cleavage activity. The kinetic parameters shown in Figure 5B were measured in 50 mM MES (pH 6.5) and 25 mM $MgCl_2$, either in the presence or in the absence of 500 μM $CdCl_2$, under multiple-turnover conditions at 37 °C. In this measurement, reaction was initiated by the addition of substrate to a buffered solution that contained the ribozyme together with the metal ions, and each resultant mixture was then incubated at 37 °C. In time course plots shown in Figure 6, reaction rates were measured in 10 mM $MgCl_2$ and 50 mM Tris-HCl (pH 8.0), either (i) under ribozyme-saturating (single-turnover) conditions at 0 °C (Figure 6A; the concentrations of ribozyme and substrate were 600 and 60 nM, respectively) or (ii) under substrate-saturating (multiple-turnover) conditions at 0 °C (Figure 6B; the concentrations of ribozyme and substrate were 60 and 600 nM, respectively). The plot shown in Figure 6A was obtained by computer-fitting to the following equation:

$$F(t) = a[1 - \exp(-b \times 10^t)] + c[1 - \exp(-d \times 10^t)]$$

In this equation, a and c indicate the endpoints of the first and second curves, respectively. The value of a was 0.46, and the value of c was 0.35. The value of k_{obs} in the first curve (which means *S*p-mediated cleavage) was determined as 0.56 min^{-1}. The value of k_{obs} in the second curve (which means *R*p-mediated cleavage) was determined as 0.0019 min^{-1}.

(14) (a) Forster, A. C.; Symons, R. H. *Cell* **1987**, *49*, 211−220. (b) Kaper, J. M.; Tousignant, M. E.; Steger, G. *Biochem. Biophys. Res. Commun.* **1988**, 154, 318−325. (c) Navarro, B.; Flores, R. *Proc. Natl. Acad. Sci. U.S.A.* **1997**, *94*, 11262−11267. (d) Kawasaki, H.; Eckner, R.; Yao, T.; Taira, K.; Chiu, R.; Livingston, D. M.; Yokoyama, K. K. *Nature* **1998**, *393*, 284−289. (e) Kuwabara, T.; Warashina, M.; Kato, Y.; Kawasaki, H.; Taira, K. *J. Biochem. Mol. Biol.* **2001**, *34*, 51−58. (f) De la Pena, M.; Flores R. *J. Biol. Chem.* **2001**, *276*, 34586−34593.
(15) Eckner, R.; Ewen, M. E.; Newsome, D.; Gerdes, M.; DeCaprio, J. A.; Lawrence, J. B.; Livingston, D. *Genes Dev.* **1994**, *8*, 869−884.
(16) Natamatsu, Y.; Warashina, M.; Kuwabara, T.; Tanaka, Y.; Yoshinari, K.; Taira, K. *Genes Cells* **2000**, *5*, 603−612.

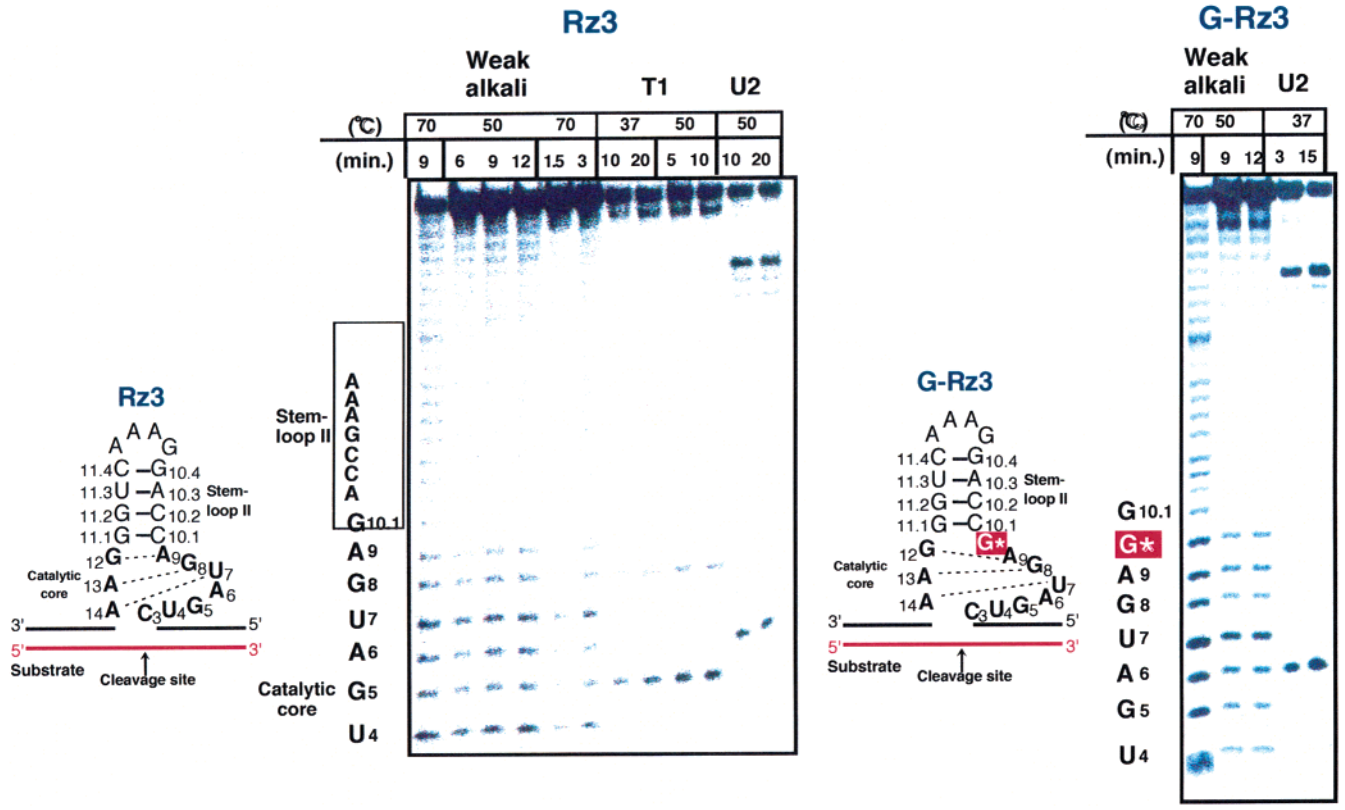

Figure 3. Probing of the secondary structures of ribozyme and G-inserted ribozyme with alkaline solution, and RNase T1 and U2, in the presence of noncleavable DNA oligomer. Single-stranded RNA is more cleavable in alkaline solution.

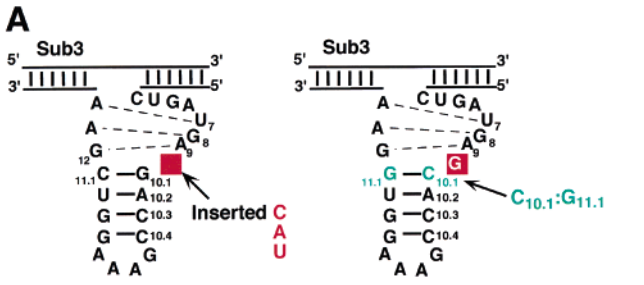

	C-Rz3	A-Rz3	U-Rz3	$C_{10.1}$:$G_{11.1}$-Rz3
k_{obs} (min^{-1})	1.02	0.78	2.1	0.02 *

Figure 4. (A) Secondary structures of different nucleotides inserted into Rz3, instead of G*. (B) Comparison of the cleavage rates of mutant G-Rz3. Rate constants were measured under multiple-turnover conditions, except that the rate constant of G10.1:C11.1-Rz3 (0.02*) was measured under single-turnover condition due to its low cleavage activity.

Reactions were stopped at intervals by removing aliquots from the reaction mixture and mixing them with an equal volume of a solution that contained 100 mM EDTA, 9 M urea, 0.1% xylene cyanol, and 0.1% bromophenol blue. The substrate and the products of the reaction were separated by electrophoresis on an 8−15% polyacrylamide/7 M urea denaturing gel and were detected by autoradiography. The extent of cleavage was determined by quantitation of radioactivity in the bands of substrate and products with a Bio-Image Analyzer (BAS2000; Fuji Film, Tokyo). All kinetic measurements were performed at least in duplicate, and the reported kinetic parameters are the average values, in that potential errors were found to be 10% for each measurement.

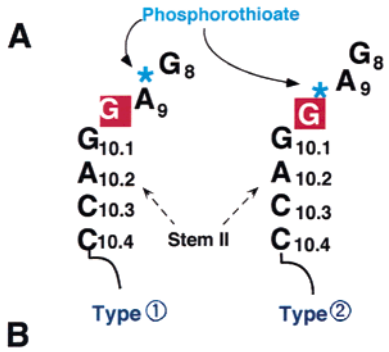

Ribozymes	k_{obs} (min^{-1}) [Ⅰ] Mg	k_{obs} (min^{-1}) [Ⅱ] Mg+Cd	Ratio: [Ⅱ] / [Ⅰ]
G-Rz3	0.37	1.6	4.3
G-Rz3S (Type ①)	0.14	2.1	15
G-Rz3S (Type ②)	0.25	1.1	4.4

Figure 5. (A) G-Rz containing a phosphorothioate-linkage at the sites indicated by asterisk. Phosphorothioate linkage are inserted between G8 and A9 (Type ①), and between A9 and the inserted-G (Type ②). (B) Effects of thio-substitution for Type ① or Type ② G-Rz on the cleavage reaction in the presence and absence of Cd^{2+}.

Probing of the Secondary Structures of Natural and Mutant Ribozymes. To evaluate the structures of Rz, we used a weakly alkaline solution, in which phosphodiester bonds in single-stranded regions were more susceptible to alkaline attack than those within double-stranded regions.[16,17] The reaction mixture for hydrolysis contained 50 mM Na_2CO_3/$NaHCO_3$ (pH 9.2), 25 mM $MgCl_2$, and 5′-^{32}P-labeled Rz (10

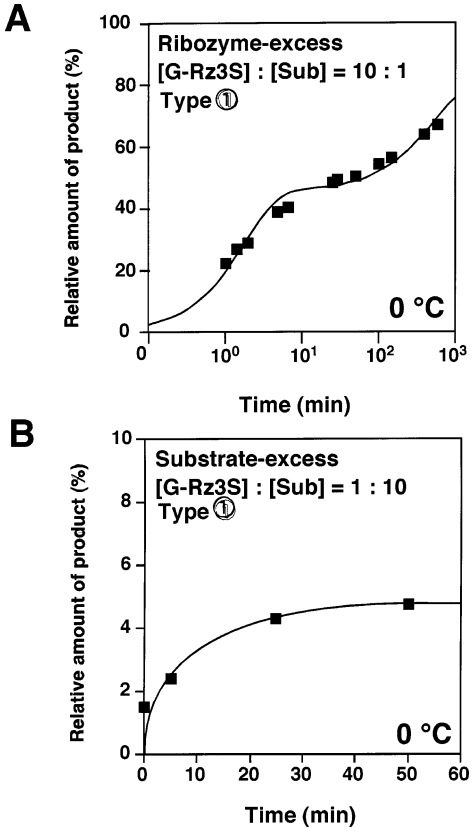

Figure 6. (A) Biphasic reactions are observed by a mixture of the thio-P9*S*p and thio-P*R*p ribozymes. (B) Burst kinetics of the reaction catalyzed by thio-substituted G-ribozymes. The ratio of the concentration of each ribozyme to the substrate is 1:10.

kcpm). The 5′-^{32}P-labeled Rz was first heated to 95 °C for 2.5 min, slowly cooled to room temperature, and allowed equilibrate for 30 min to avoid formation of local minimum-energy structures. The concentrations of the ribozyme and the uncleavable substrate, which is 13mer DNA corresponding to RNA substrate, were 10 nM (10 kcpm) and 6 μM, respectively. The reactions were initiated by the addition of the alkaline solution, with incubation at 37, 50, or 70 °C. All reactions were quenched by quickly freezing the reaction mixtures after the addition of an equal volume of a solution of 7 M urea, 100 mM EDTA, 0.1% xylene cyanol, and 0.1% bromophenol blue.

To make control ladders, we also used RNase T1, which cleaves at G residues in single-stranded regions, and RNase U2, which cleaves at A residues in single-stranded regions. 5′-^{32}P-Labeled Rz (10 kcpm) was digested with 0.01 U of RNase T1 in 50 mM Tris-HCl (pH 7.5) with 25 mM Mg^{2+} ions. 5′-^{32}P-Labeled Rz (10 kcpm) was digested with 0.5 U of RNase U2 in 20 mM sodium citrate (pH 4.5) with 25 mM Mg^{2+} ions. Prior to the RNase-mediated cleavage of RNA, Rz was incubated with its uncleavable substrate. The concentration of each RNA was the same as that in the experiments with the weakly alkaline solution. All reactions were quenched as described above. The partially digested ribozymes were fractionated on a 20% polyacrylamide/7 M urea denaturing gel. Fragments on gels were identified from their mobilities.

Results and Discussion

Mutant G-Inserted Ribozymes and Their Activities. There have been several attempts to determine both the overall global structure and the detailed atomic structure of the hammerhead ribozyme. The X-ray crystal structures determined by McKay's group and Scott's and Klug's group are nearly identical in terms of tertiary folding and conformation.[18a−c] In the X-ray structure (Figure 1A) the catalytic core is divided into two regions: domain I consisting of $C_3U_4G_5A_6$ and domain II consisting of nucleotides $G_{12}A_{13}A_{14}$ and $U_7G_8A_9$. The nucleotides of domain II form two sheared G:A base pairs between G_8:A_{13} and A_9:G_{12} and a non-Watson−Crick A_{14}:U_7 base pair that consists of one hydrogen bond (these interactions are indicated by dotted lines in Figure 1). This extended stem II stacks onto the non-Watson−Crick base pair, $A_{15.1}$:$U_{16.1}$, resulting in formation of a pseudo-A-form helix by stems II and III (Figure 1A, left).[18] The adjacent non-Watson−Crick A−U base pairs (A_{14}:U_7 and $A_{15.1}$:$U_{16.1}$) form the basis of a three-way junction. The four nucleotides ($C_3U_4G_5A_6$) of domain I form a "uridine-turn" motif, allowing the phosphate backbone to turn and connect with stem I.

During the construction of ribozyme vectors, we isolated an active mutant ribozyme that had an extra G residue inserted between A9 and G10.1 of the consensus catalytic core (Figure 1B).[5d,14d,e] The G-inserted mutant ribozymes had high activities in vitro and in vivo, and they appeared indistinguishable from the parental ribozymes. In the case of our mutant G-inserted ribozymes (G-Rz), the pseudo-A-form helix formed by stems II and III should be perturbed by the insertion of a G residue (Figure 1B),[5d,14d,e] as should be for the naturally occurring extra nucleotide-inserted ribozymes.[14a−c,f] To demonstrate the general activity of the extra nucleotide-inserted ribozymes, we first synthesized four G-Rz targeting four different NUX (GUX) sites[9b] within p300 mRNA,[14d] and kinetic parameters were determined under multiple-turnover conditions. The results of such kinetic measurements are summarized in Figure 2. Because of the high level of activities of G-Rz, cleavage reactions were performed under multiple-turnover conditions. From the pH−log(rate) profiles in Figure 2B, it is clear that the measured rate constants (k_{cat}) reflect the chemical cleavage step.[1] It is also true that G-Rz in general have high levels of activity. Surprisingly, the k_{cat} value of G-Rz3 was extremely high (6.4 min^{-1}). The k_{cat} value of the corresponding parental ribozyme under similar conditions is in general slightly larger than 1 min^{-1}, as indicated in Figure 2A. Our standard ribozyme (R32), which we usually use in kinetic analysis for mechanistic studies because R32 is a well-behaved ribozyme,[4] has the k_{cat} value of 2.5 min^{-1} under the conditions used in this study. To the best of our knowledge, G-Rz3 and the other U-inserted ribozyme[14f] appear to be the most active mutant ribozymes that have the natural all-RNA backbones without invoking kissing interactions.[19]

Structures of the G-Inserted Ribozymes. Despite the fact that the pseudo-A-form helix in G-Rz formed by stems II and III should be perturbed by the insertion of a G residue (Figure 1B), all G-Rz supported extremely high levels of activity. Considerable secondary structures of G-Rz with bulged-out G (inserted residue; Figure 1B, left), bulged-out G10.1 (Figure 1B, center), or bulged-out A10.2 (Figure 1B, right) are depicted

(17) Zhou, D.-M. Nakamatsu, Y.; Kuwabara, T.; Warashina, M.; Tanaka, Y.; Yoshinari, K.; Taira, K. *J. Inorg. Biochem.* **2000**, *78*, 261−268.

(18) (a) Pley, H. W.; Flaherty, K. M.; McKay, D. B. *Nature* **1994**, *372*, 68−74. (b) Scott, W. G.; Finch, J. T.; Klug, A. *Cell* **1995**, *81*, 991−1002. (c) Scott, W. G.; Murray, J. G.; Arnold, J. R. P.; Stoddard, B. L.; Klug, A. *Science* **1996**, *274*, 2065−2069. (d) Scott, W. G.; Klug, A. *Trends Biochem. Sci.* **1996**, *21*, 220−224. (e) McKay, D. B. *RNA* **1996**, *2*, 395−403. (f) Murray, J. B.; Terwey, D. P.; Maloney, L.; Karpeisky, A.; Usman, N.; Beigelman, L.; Scott, W. G. *Cell* **1998**, *92*, 665−673.

(19) Khvorova, A.; Lescoute, A.; Westhof, E.; Jayasena, S. D. *Nat. Struct. Biol.* **2003**, *10*, 708−712.

in Figure 1B. To distinguish these structures and to identify the possible active G-Rz structure, we then carried out chemical probing analysis.

In general, in studies of stem-loop structures of RNAs, divalent heavy metals, such as Pb^{2+} ions, as well as Fe(II)-EDTA, diethyl pyrocarbonate, and dimethyl sulfate, have been used in chemical probing experiments.[20] It is well known that, at high pH, all phosphodiester bonds in RNAs are cleaved rapidly because of intramolecular anchimeric attack by 2′-OH groups. We previously demonstrated that, in weakly alkaline solution, rates of hydrolysis of phosphodiester bonds in the duplex region were significantly lower, because of the rigid conformation,[21] than corresponding rates in single-stranded regions, and thus this property was used to probe the secondary structure of RNAs.[17] In view of the probable advantages of the chemical probing of functional RNAs by simple weak-alkaline hydrolysis, we performed such analysis using our maxizyme complex that consisted of four strands of RNA.[8d]

Our success with the maxizyme in probing its secondary structure by the simple weak-alkaline hydrolysis[17] led us to use the same strategy in probing the G-Rz (Figure 3). This strategy clearly distinguishes the single-stranded region from the stemmed region. In comparison with the results with the parental Rz (left), it is apparent that, in the case of G-Rz (right), the inserted G (indicated by an asterisk) locates within the catalytic core: note that the parental Rz produced six bands, corresponding to the cleavages at U4, G5, A6, U7, G8, and A9, whereas G-Rz produced seven bands in that one additional band originated from the inserted G. Therefore, the chemical probing data support that the majority of G-Rz populations remain with bulged-out G (inserted residue; Figure 1B, left), as shown in Figure 3.

Other Mutant Ribozymes and Their Activities. Our chemical probing data demonstrated that (i) the non-Watson−Crick base-pairing interactions within the catalytic core (indicated by dotted line; Figure 1), which link stem II with stem III, resulting in formation of a pseudo-A-form helix by stems II and III, are weaker than the Watson−Crick base-pairing interactions within stem II in both natural Rz and G-Rz (indicated by solid line; Figure 1) and that (ii) the inserted G locates within a weaker base-pairing region, namely, within the catalytic core. The most likely structure of G-Rz is the one with bulged-out inserted-G from the pseudo-A-form helix formed by stems II and III (Figure 1B, left, and Figure 3).

We then tested whether other nucleobases might similarly support the catalysis or the newly inserted C instead of G might rearrange the base-pairings within the catalytic core by the formation of inserted-C:G12 base-pairing with bulged-out A9, resulting in reduction of activity (Figure 4). Kinetic measurements were made, under conditions similar to those used for other G-Rz shown in Figure 2, under multiple-turnover conditions. The results of such measurements are summarized in Figure 4B, where k_{obs} most likely represents k_{cat}, namely, the rate constant of the chemical cleavage step. Apparently, the rate constants were comparable to those of G-Rz. As expected, when the natural G10.1:C11.1 base pair had been replaced by the C10.1:G11.1 base pair within G-Rz, significant reduction of the activity was realized. It has been known in the literature that such G10.1:C11.1-to-C10.1:G11.1 mutation within natural hammerhead ribozymes significantly hampers the catalysis, supporting the importance of the P9-G10.1 motif.[12]

The Importance of P9 Phosphate within G-Rz. All the available data are pertinent to the structure with bulged-out inserted base from the pseudo-A-form helix formed by stems II and III. The next question, then, is whether the position of the catalytically important P9 phosphate, especially the *pro-R*p oxygen, might have changed from the original phosphate between G8 and A9 to the adjacent phosphate between A9 and the inserted G (Figure 5A). Most studies of crystal structures of Rz have identified a metal-binding site between the *pro-R*p oxygen of the phosphate of A9 and the N7 atom of G10.1.[3,10,11] Even though this metal-binding site (P9 site) within the crystal structure is located approximately 20 Å from the scissile phosphodiester bond, this metal-binding site is thought to play a crucial role in achieving maximal cleavage activity for the following reasons. The substitution of the *pro-R*p phosphoryl oxygen at P9 by a sulfur atom (in the P9-*R*pS ribozyme) resulted in a decrease in Mg^{2+}-dependent catalytic activity.[22] Moreover, from the kinetic studies of P9-*R*pS Rz, it was demonstrated that the *R*p phosphorothioate linkage reduced the cleavage rate by a factor of 10^3. However, the rate returned to the control value after the addition of a low concentration of Cd^{2+} ions, which are thiophilic.[23,24]

To identify the important phosphate within G-Rz, we synthesized two types of phosphorothioate-containing G-Rz3S (Figure 5); the kinetics of those mutants should answer the question of whether the position of the catalytically important P9 phosphate might have changed from the original phosphate between G8 and A9 (Figure 5A, left; type ①) to the adjacent phosphate between A9 and the inserted G (Figure 5A, right; Type ②). The position of the phosphorothioate linkage is indicated by the asterisk in Figure 5A. We note that G-Rz3S is a diastereomeric mixture of *R*p and *S*p phosphorothioate configurations (G-Rz3S with *R*p and *S*p phosphorothioate linkages in a 1:1 ratio).

To follow the reactions more accurately, a lower pH of 6 was used in this kinetic study. By the introduction of the phosphrothioate linkage, both types of G-Rz3S reduced the activity; the activity of Type ① was hampered more significantly. In general, addition of Cd^{2+} ions enhances ribozyme activities because the pK_a of the hydrated Cd^{2+} ion is lower than that of Mg^{2+} ion and, thus, Cd^{2+} ions can better catalyze the Rz-mediated cleavage reactions than Mg^{2+} ions.[4,10b] The

(20) (a) Milligan, J. F.; Uhlenbeck, O. C. *Methods Enzymol.* **1989**, *180*, 51−64. (b) Pan, T.; Uhlenbeck, O. C. *Nature* **1992**, *358*, 560−563. (c) Bernal, J. J.; Garcia-Arenal, F. *RNA* **1997**, *3*, 1052−1067. (d) Felden, B.; Himeno, H.; Muto, A.; McCutcheon, J. P.; Atkins, J. F.; Gesteland, R. F. *RNA* **1997**, *3*, 89−103. (e) Ushida, C.; Sasamura, S.; Muto, A. *J. Biochem.* **1997**, *122*, 1202−1207. (f) Costa, M.; Christian, E. L.; Michel, F. *RNA* **1998**, *4*, 1055−1068. (g) McGregor, A.; Murray, J. B.; Adams, C. J.; Stockley, P. G.; Connolly, B. A. *J. Biol. Chem.* **1999**, *274*, 2255−2262. (h) Phillips, C.; Kyriakopoulou, C. B.; Virtanen, A. *Nucleic Acids Res.* **1999**, *27*, 429−438.

(21) Zagórowska, I.; Kuusela, S.; Lönnberg, H. *Nucleic Acids Res.* **1998**, *26*, 3392−3396.

(22) Ruffner, D. E.; Stormo, G. D.; Uhlenbeck, O. C. *Biochemistry* **1990**, *29*, 10695−10702.

(23) Perracchi, A.; Beigelman, L.; Scott, E. C.; Uhlenbeck, O. C.; Herschlag, D. *J. Biol. Chem.* **1997**, *272*, 26822−26826.

(24) In our recent NMR studies by using the metal-binding motif of A9/G10.1 site (ref 11c,d), we found that the substitution of the oxygen atom with a sulfur atom at *pro-R*p position of A9 (P9 site) could change the conformation of the natural ribozyme and this conformational change may cause the reduction of the catalytic activity (Suzumura et al., manuscript in preparation). This NMR study casts a question as to the important role of *pro-R*p oxygen.

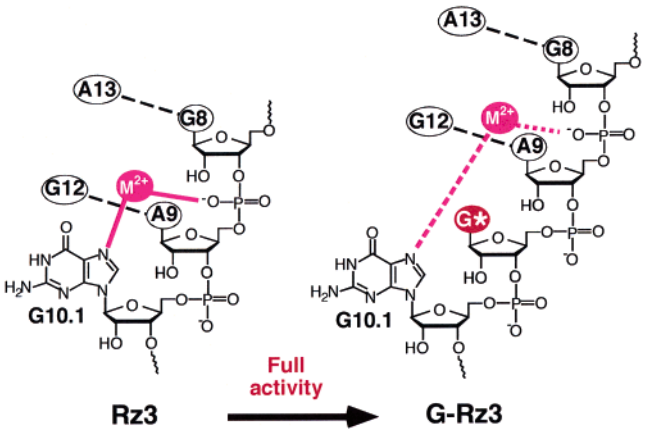

Figure 7. Schematic models of the interaction between Mg^{2+} and the region around G10.1 and A9 phosphate. Even a insertion of a G nucleotide between A9 and G10.1 retains full catalytic activity. Since introduction of phosphorothioate at P9 site is very sensitive (Figure 5), and since the mutant C10.1:G11.1 G-inserted ribozyme was inactive (Figure 4B), the metal ion appears to coordinates with P9 phosphate and the G10.1 base (right).

intrinsic enhancement by the addition of Cd^{2+} ions to the G-Rz3-catalyzed reactions was 4.3-fold (Figure 5B). Similar enhancement was realized in the case of Type ② G-Rz3S with 4.4-fold increase in rate by the addition of Cd^{2+} ions. By contrast, the increase in rate (15-fold increase) of Type ① G-Rz3S-catalyzed reactions was significantly higher than that of the other two cases, implicating an additional interaction between the thiophilic Cd^{2+} ion and the introduced sulfur atom at the original P9 site between A9 and G8. Therefore, the more significant thio effect (reduction in k_{obs} from 0.37 to 0.14) and the observed rescue by the thiophilic Cd^{2+} ion in the case of Type ① G-Rz3S suggest that the original P9 site plays an essential role for the capture of the important divalent ions, even in the case of an extra nucleotide-inserted ribozymes.[5d,14]

To analyze in further detail the importance of P9 phosphate, kinetic studies were carried out under single-turnover (Figure 6A) and multiple-turnover (Figure 6B) conditions at 0 °C; at this low temperature, substrate dissociation from the ribozyme−substrate complex is negligible.[23,25] In the case of ribozyme-excess single-turnover conditions, all the substrates were at first bound with the Type ① G-Rz3S. Under the conditions of the measurements, we could follow the chemical cleavage step of a single-turnover reaction, leading to a biphasic kinetics as shown in Figure 6A. As described in the Experimental Section, rate constants for the fast and slow reactions can be estimated to be 0.56 and 0.0019 min^{-1}, respectively, for the *S*p- and *R*p-catalyzed reactions.[22,23]

We then followed the kinetics under substrate-saturating multiple-turnover conditions (Figure 6B), with the ribozyme (Type ① G-Rz3S) to its substrate ratio of 1:10. At first, all the Type ① G-Rz3S with *R*p and *S*p phosphorothioate linkages in the 1:1 ratio were bound with the substrates. Under this condition, 90% of the substrates were unbound because of the substrate-excess conditions. Kinetics were followed at 0 °C, and Figure 6B demonstrates that half of the bound substrates (5% of the total substrates) could be cleaved within 60 min, most probably by the G-inserted Rz with the *S*p phosphorothioate configuration. The remaining half of the *R*p phosphorothioate-bound substrates (5% of the total substrates) remained uncleaved under this condition.

Taken all together, the more than 2 orders of magnitude difference in the two kinetic parameters is attributable to the difference of the cleavage activities between *R*p and *S*p phosphorothioate conformers at the P9 site of the G-inserted riobozyme. These results are consistent with the previous observations with the natural ribozyme[22,23] that the rate of the first phase is caused by *S*pS and the second by *R*pS ribozymes. Therefore, the present data support the idea that the active structure of the G-Rz is the one shown on the right side of Figure 7.

Conclusion. To date, no structural data exist regarding the important P9-G10.1 metal-binding motif for the naturally occurring, extra nucleotide-inserted ribozymes.[14] In this study, we could propose a structural model (Figure 7, right) by analyzing highly active G-Rz and its derivatives. Since (i) the substitution of the phosphoryl oxygen at the original P9 site between G8 and A9 by a sulfur atom within G-Rz resulted in a decrease in Mg^{2+}-dependent catalytic activity and it was rescued by the addition of Cd^{2+} ions and (ii) biphasic kinetics were observed for the *R*p and *S*p phosphorothioate conformers at the P9 site of the G-inserted riobozyme, it is apparent that the original P9 phosphate plays an important role in reactions catalyzed by G-Rz (Figure 7, right). Since the mutant C10.1:G11.1 G-inserted ribozyme was inactive (Figure 4B), the metal appears to coordinate with G10.1 base (Figure 7, right). The chemical probing data suggested that the most likely structure of G-Rz is the one with bulged-out inserted-G from the pseudo-A-form helix formed by stems II and III (Figure 1B, left, and Figure 3). It is in a sense surprising that the present G-Rz and other such naturally occurring extra nucleotide-inserted ribozymes could maintain the full catalytic activities despite the perturbation of the pseudo-A-form helix formed by stems II and III, and that one extra nucleotide inserted between A9 and G10.1 would still support the function of the P9-G10.1 metal-binding motif (Figure 7, right). Clearly, the P9-G10.1 motif is one of the most important regions not only in the natural ribozyme but also for the extra nucleotide-inserted other ribozymes. Our results (Figure 7) appear to suggest the existence of an alternative structure(s) that fully support the Rz-mediated catalysis. This interpretation is consistent with our recent conclusion that the P9-G10.1 metal-binding motif is relatively flexible so that both hydrated and unhydrated metal ion(s) can be captured by this motif.[11d]

JA049634M

(25) (a) Takagi, Y.; Taira, K. *FEBS Lett.* **1995**, *361*, 273−276. (b) Warashina, M.; Takagi, Y.; Sawata, S.; Zhou, D. M.; Kuwabara, T.; Taira, K. *J. Org. Chem.* **1997**, *62*, 9138−9147.